ISSN: 2093-5374 / E-ISSN: 2093-5382

# Design and Analysis of Wireless Power Transmission (2X1) MIMO Antenna at 5G - Frequencies for Applications of Rectenna Circuits in Biomedical

Ahmed Abdul-Kadhem Salih[1*], and Mahdi Nangir[2]

[1*]Faculty of Electrical and Computer Engineering, University of Tabriz, Tabriz, Iran.
ahmed.kadhem301@gmail.com, https://orcid.org/0009-0007-7196-026X

[2]Faculty of Electrical and Computer Engineering, University of Tabriz, Tabriz, Iran.
nangir@tabrizu.ac.ir, https://orcid.org/0000-0002-1926-743X

Received: April 10, 2024; Revised: June 22, 2024; Accepted: August 02, 2024; Published: September 30, 2024

## Abstract

This research presents the design and analysis of a 5G harvesting energy Circuit (MIMO-rectenna) to receive wireless power at Sub-6 frequencies (5.6 GHz) as a power source for some medical devices carried by a patient and moved from one place to another, whether they are diagnostic or therapeutic devices. This concept aims (MIMO-rectenna) to increase the likelihood of obtaining electricity from the ambient field by harvesting energy at 5G- frequencies. The tiny MIMO (2x1) antenna measuring 30 by 40 mm2 is the antenna portion of this rectenna. It has been built and tested to operate at Sub-6 frequency, or 5.6 GHz, for wireless power transmission applications related to 5G technology. The MIMO antenna has parameters of E = 4.4, h = 1.6 mm, and tand = 0.025 when printed on an FR4 substrate. A significant section of the antenna's rear was removed to carry out the broadband process, and the material's front side was composed of a series of circular slits. In this antenna, the parasitic approach was employed to decrease the mutual coupling between two ports by creating an inverted T with precise dimensions. The CST software 2024 was used to assist with the design and simulation results of this MIMO antenna. It was discovered through the simulation that the mutual coupling for these ports, $S_{12}$and $S_{21}$, is equal to -51.476 dB, and that the S-parameters, $S_{11}$, $S_{22}$, equal -22 dB. That is, there is very little signal loss while switching from the first port to the second and vice versa. This antenna's rectifier comprised an AC-to-DC conversion circuit, a DC filter, and an impedance-matching network. With the use of ADS software 2024, this rectenna's design and simulation results were completed. The greatest conversion efficiency of this rectenna at the frequency of 5.6 GHz is determined to be between 65 % and 65.01% for load resistance between 12 KΩ and 15 KΩ at an input power of 14 dBm.

**Keywords:** Rectenna, HSMS-282B Schottky Diode, Conversion Efficiency, MIMO Antenna, Mutual Coupling, Fifth Generation (5G), Impedance Matching Networks (IMN), Dc. Filter, Parasitic Method and Wireless Power Transmission.

## 1 Introduction

In the last two decades, wireless communication systems have received unrivalled growth and have been developed from analogue to digital signals due to the modern techniques that increase their performances (Dahri et al., 2017). The main demands of the researchers in this field are to get, discover

*Journal of Wireless Mobile Networks, Ubiquitous Computing, and Dependable Applications (JoWUA),* volume: 15, number: 3 (September), pp. 203-221. DOI: *10.58346/JOWUA.2024.I3.014*

*Corresponding author: Faculty of Electrical and Computer Engineering, University of Tabriz, Tabriz, Iran.

and propose novel techniques that provide very good benefits (unique advantages) such as increasing the data rate transfer, increasing the level of diversity and decreasing the probability of error, etc., and this is the real reason for the emergence of generations and their evolutions in wireless networks (Wu et al., 2013; Dahri et al., 2017; Kim, 2020). Using multi-input multi-output (MIMO) technology has advanced modern wireless communication systems to a new stage of development. This is because higher data rates result in higher channel capacity and dependability as well as a lower chance of error. Masoodi et al., (2021) The majority of modern mobile terminals use printed antennas that leverage the device's system ground plane. As a result, printed antennas are inexpensive, simple to fabricate, and can be tailored to the specifications of the device (Ramakrishna et al., 2021; Zhu et al., 2021). MIMO-based mobile devices for wireless communication rely on integrated multiple antennas (Ramakrishna et al., 2021; Gaurav et al., 2018). MIMO-based wireless communication devices rely on multiple antennas that are integrated within the mobile device (Alkaraki & Gao, 2020; Ram & Chakraborty, 2024). The use of multiple antennas can increase data rate and thus provide users with more multimedia, real-time video connectivity, and data transfer capabilities (Masoodi et al., 2021; Hussain et al., 2019). All upcoming wireless generations will employ MIMO technology, hence for the system to reach the high data rates that are anticipated, the antenna component of the system needs to be carefully built and characterized. (Khan et al., 2020; Abdalla & Ibrahim, 2017).

Since semiconductor technology has advanced, wireless electronic devices have become increasingly common (Wu & Ma, 2013; Rajesh et al., 2023). These devices require little power and are typically battery-powered, which has drawbacks such as the need for constant maintenance due to the battery's short lifespan and increased cost when operating in harsh environments (Bobir et al., 2024). As a solution, ambient power harvesting techniques have been proposed. A rectenna is a device that transforms microwave energy into direct current (DC) electricity (Ibrahim et al., 2022; Zhu et al., 2021) is a rectifying antenna, which functions without an internal power supply by combining an antenna with a nonlinear rectifying device (Schottky diode, IMPATT diode, etc.) (Muhammad et al., 2020). Figure 1 displays the rectenna schematic diagram. The selection of the working frequency in a rectenna design is contingent upon its intended application (Ibrahim et al., 2022; Prabhu et al., 2013). As frequency increases, the amount of power that an antenna receives at a given distance from the emitter drops. Friis equation provides the available power (Pr) at a certain distance from the emitter (Hussain et al., 2019; Prabhu et al., 2013). The equation (1) is given as,

$$P_r = P_t . G_t . G_r . \left(\frac{\lambda}{4\pi R}\right)^2 \quad (1)$$

Where λ is the wavelength being used, R is the distance between the transmitter and the receiver, $G_t$ and $G_r$ are the transmitter and receiver antenna gains, and $P_t$ is the transmitter power (Sanad & Hassan, 2014).

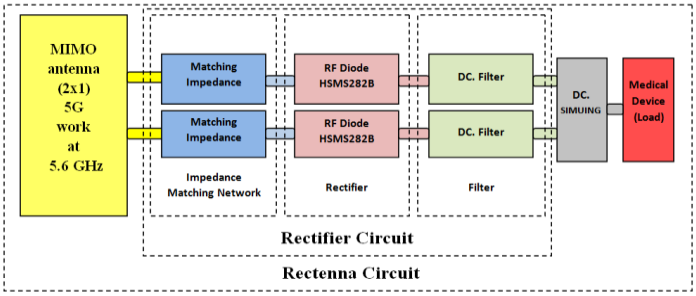


Figure 1: Block Diagram of a Rectenna

In 1964, the rectenna was invented and later patented in 1969 by William C. Brown, an electrical engineer from the United States (Brown, 1984). Brown demonstrated the technology using a model aircraft powered by microwaves, which were transmitted from the ground and received by an attached rectenna. Since the 1970s, a significant driver of rectenna research has been the development of receiving antennas for solar power satellites. These satellites would collect sunlight in space using solar cells and beam the energy down to Earth as microwaves, which would be captured by large rectenna arrays (Wu et al., 2013). Two rectenna circuits were designed for operation at 2.45 GHz and 35 GHz (McSpadden et al., 1992). They achieved efficiencies of 85% at 1.2 W input power and 29% at 120 mW input power, respectively. In another study, a compact rectenna circuit with an output voltage of 50 V—suitable for powering mechanical actuators—was introduced (Epp et al., 2000). The circuit used double rectenna elements to boost the output voltage. Additionally, a small circularly polarized rectenna was designed to operate at 5.5 GHz, incorporating a built-in band-reject filter to suppress out-of-band harmonics at 11 GHz (Ali et al., 2006). This rectenna demonstrated more than 50 dB of harmonic suppression and a conversion efficiency of 74%. A compact circularly polarized patch antenna rectenna with an RF-to-DC power conversion component operating at 2.45 GHz was also proposed. The selected antenna, built on a low-cost FR4 substrate, had a measured bandwidth of 137 MHz and a circular polarization bandwidth of 30 MHz (3 dB axial ratio). With a 1 KΩ load resistor, the RF-to-DC conversion efficiency reached 75% (Yo et al., 2008). Furthermore, a small, programmable rectenna operating at 5.2 GHz and 5.8 GHz for wireless power transfer was developed. The simulated efficiencies for input power of 16.5 dBm were calculated as 70.5% and 69.4%, respectively (Lu et al., 2014). Another circularly polarized rectenna with harmonic suppression, designed to operate at 5.8 GHz, achieved a bandwidth of 31.8% for wireless power transfer applications (Yang et al., 2018). A quartz clock was also developed, incorporating wireless energy harvesting and sensing capabilities. Its rectifier was optimized to rectify the power captured by matching directly with the clock antenna, with a maximum efficiency of 65% achieved within the 1.4–1.5 GHz and 1.9–2.1 GHz frequency ranges (Song et al., 2018). Mobile Phone Generation Bands and Features shown in Table 1.

Table 1: Mobile Phone Generation Bands and Features (European 5G Observatory; Babu et al., 2011).

| Properties | $1^{st}$ generation | $2^{nd}$ generation | $3^{rd}$ generation | $4^{th}$ generation | $5^{th}$ generation |
|---|---|---|---|---|---|
| Appearing year | 1980s | 1988s | 2006s | 2010s | 2020s |
| Radio signals | analogue | digital | digital | digital | digital |
| Customized for | Voice call and text message | Voice call and text message | Voice call and text message and video | Voice call and text message and video | Voice call and text message and video |
| Technique | AMPS | GSM | HSPA, WCDMA | LTE(MIMO)WiMAX | LTE(MIMO)WiMAX |
| Weight | Heavy | Light | Mire light | Very light | Very light |
| Frequency band | 850 MHz | 900/1800MHz | 900/1800 2100/2600 MHz | 900/1800 2100/2600 3500 MHz | 900/1800 2100/2600 3500 [ Sub-6 (3.3-6) GHz & mm-wave (23-40) GHz] |
| Upload data rate | Very few data rate | 56 Kbps,118 Kbps | 384Kbps,5.7Mbps | 75 Mbps | 20Gbps |

In the field of medical devices today, A large number of medical devices are being discovered that help people get rid of their diseases or relieve their pain. Some of them may be portable devices on the patient's body, such as the electronic pancreas and Holter ECG. In addition, a large number of devices are implanted in patients' bodies to carry out certain tasks, such as controlling their heartbeat, and these devices need energy to function, which comes from batteries. Exposure results from the process needed to remove and recharge these batteries when their energy runs low. Through a wireless communication mechanism between the devices and the surrounding signals, such as telecom or Internet signals and other signals that have the same frequency as the medical device, the Rectenna devices function to provide electrical energy to the batteries of medical equipment (Andrea, 2013; Zhang et al., 2014). This leads to reducing the risk to the patient during operations and his comfort in using it. Some Medical Devices Require Portable DC Power shown in Figure 2.

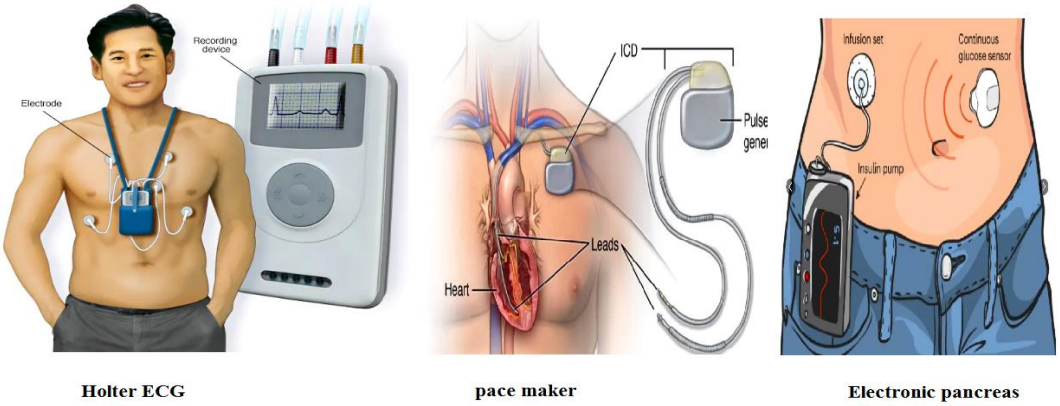


Figure 2: Some Medical Devices Require Portable DC Power

## 2 Antenna Design

In this paper, the proposed antenna is a monopole antenna consisting of two ports operating at frequency Sub-6 frequency 5.6 GHz compact size (30×20) $mm^2$. The focus of this antenna is to design the parasitic to reduce the mutual coupling between the two ports. There are two cases to study the effect of plastic in reducing the mutual coupling between the two antennas:

**Case one** the antenna was designed without a parasitic separating the two ports, as in Figure 1 to see the extent of the effect of the mutual coupling between the two ports and the S-parameter. Printed MIMO Antenna Without Parasitic shown in Figure 3.

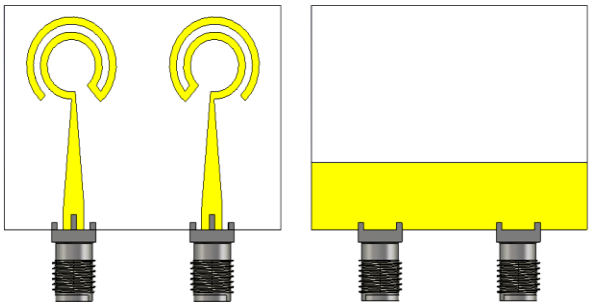

(a) (b)

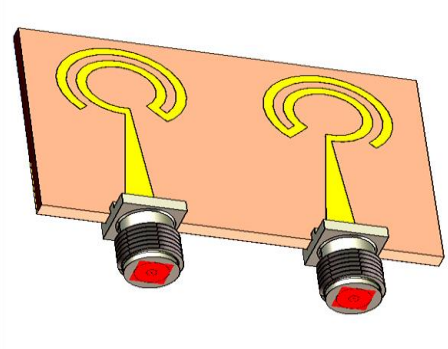

(c)

Figure 3: Printed MIMO Antenna Without Parasitic

(a) Top View (b) Back View (c) 3D View

Figure 4 shows that S - parameter for each $S_{11}$, $S_{22}$ eual -16 dB , $S_{12}$and $S_{21}$ equal -14 dB It has a signal of less than 10 dB at frequency 5.6 GHz, which makes the antenna able to receive a signal well, and the loss of the signal as a result of its transmission from the first to the second port and vice versa is also small, but when using the antenna in rectenna, the antenna needs to harvest the energy surrounding it with the largest possible signal, and the loss of the signal is due to mutual coupling as little as possible.

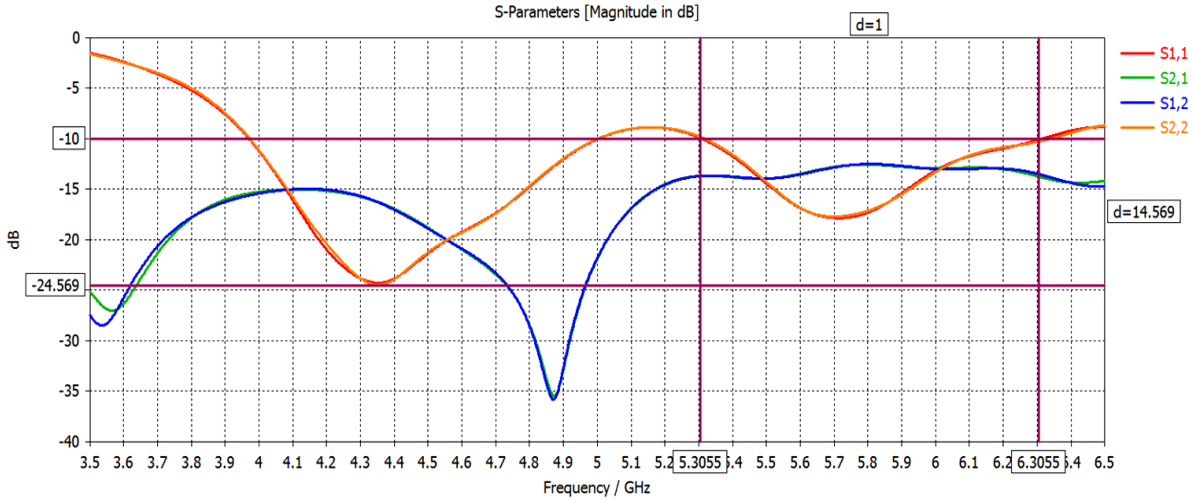


Figure 4: S - parameter without Parasitic

Figure 5 shows the isolation between the two ports, as some of the signals move from the first port to the second and vice versa in a large proportion, this will lead to an increase in mutual coupling because no spacer between them prevents the transmission of that antenna, in this case, is weak in the performance of work.

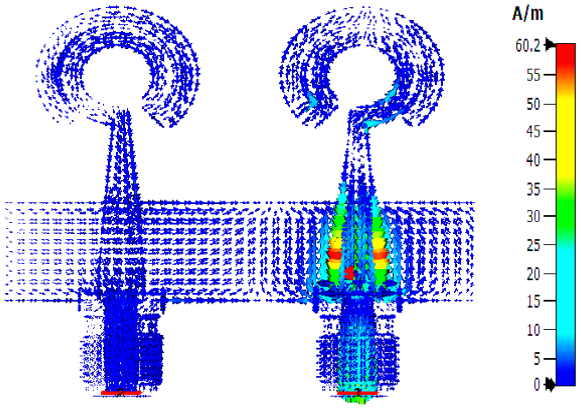


(a)

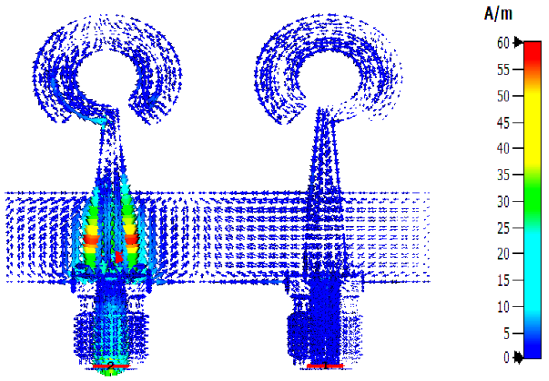


(b)

Figure 5: Current Distribution (Surface Current) MIMO Antenna Without Parasitic

a) Port 1 (b) Port 2

**Case two** parasitic is designed in the front face of the antennas in the form of a letter T upside down in the middle, as shown in Figure 6. Its usefulness is to reduce the signal exchange between the two antennas to prevent lost signal losses as a result of this exchange and to send the signal with the largest possible energy. Printed MIMO Antenna with s Parasitic Shown in Figure 7. The Optimum Design Dimensions of Parasitic MIMO Antenna shown in Table 2.

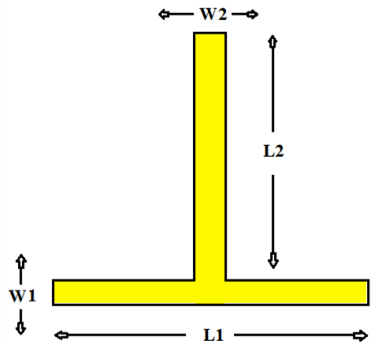


Figure 6: Dimension of Parasitic

Table 2: The Optimum Design Dimensions of Parasitic MIMO Antenna

| Material type | Copper |
|---|---|
| Conductor thickness | 0.035 mm |
| L1 | 10 mm |
| L2 | 10.615 mm |
| W1 | 0.5 mm |
| W2 | 0.6 mm |

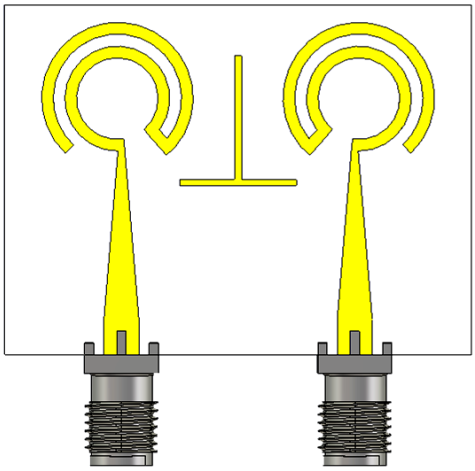

Figure 7: Printed MIMO Antenna with s Parasitic

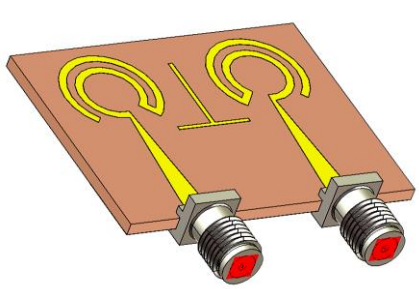

(a)

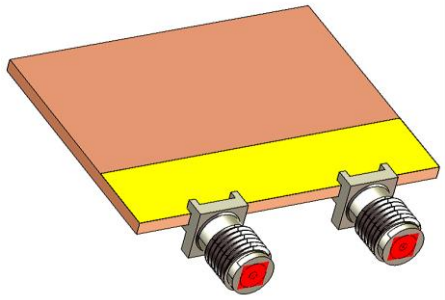

(b)

Figure 8: Printed MIMO Antenna with Parasitic (a) 3D Top View (b) 3D Back View

Figure 8 shows that the S- parameter for each $S_{11}$, $S_{12}$ ,$S_{21}$and $S_{22}$ after adding a parasitic. S - parameter for each $S_{11}$, $S_{22}$ equal - 23 dB ,$S_{12}$and $S_{21}$ equal - 51.545 dB, at frequencies from 5.6 GHz. The results of the antenna after adding the parasitic are much better than before adding the parasitic in terms of loss of signal energy transmitted from the first port to the second port and vice versa. Also, the antenna can harvest the energy surrounding it as much as possible in the first case. S - Parameter with Simple Parasitic shown in figure 9.

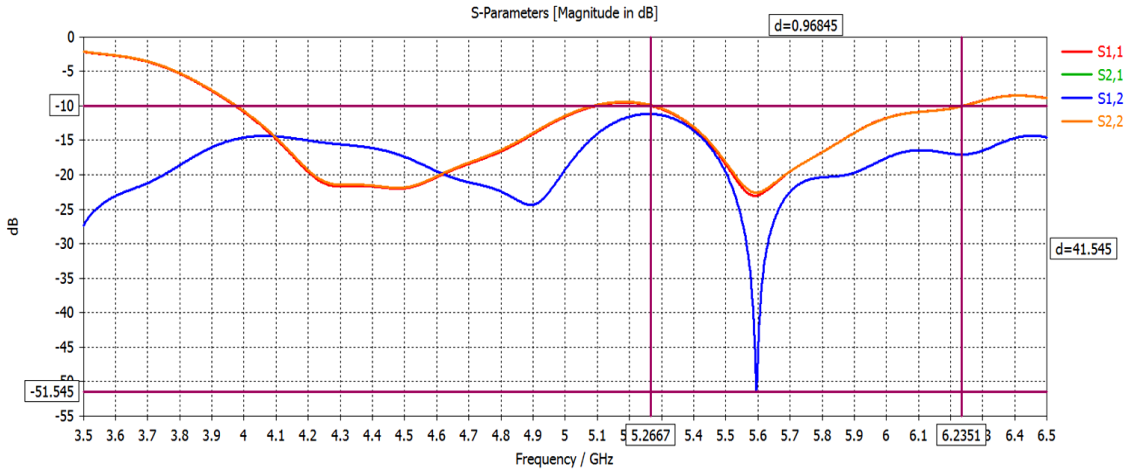


Figure 9: S - Parameter with Simple Parasitic

The mutual coupling as shown in Figure 10 has become less than the first case. The method of designing the parasitic led to the prevention of the exchange of signals between the two antennas, and improvement in the signal of the S- S-parameter in general and this is what we aspire to reach.

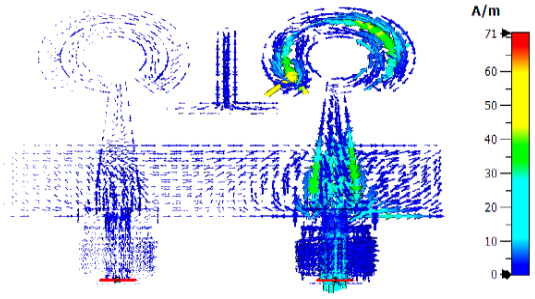


(a)

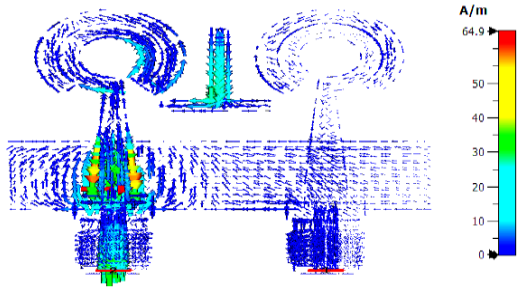


(b)

Figure 10: Current Distribution (Surface Current) MIMO Antenna with Parasitic: (a) Port 1 (b) Port 2

# 3 Simulation of Antenna Design

### 1) Reflection Coefficient

The reflection coefficient is defined as the ratio of the power reflected to the source (Pr) to the power transmitted from the source (Pi). When broadcasting from a transmitter to an antenna, the power loss can be calculated by computing the reflection coefficient (Wu & Ma, 2013). The reflection coefficient values (in dB) as a function of frequency are displayed in Figure 11.

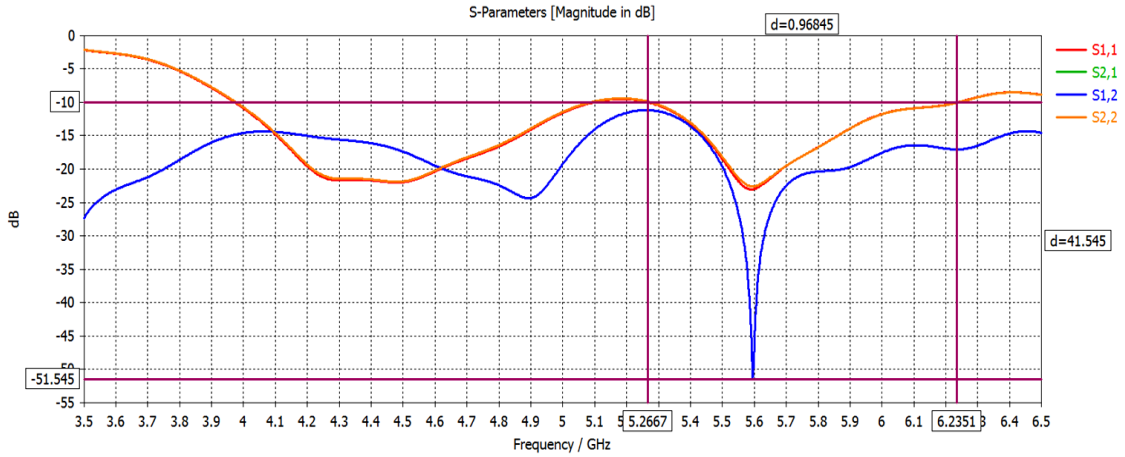


Figure 11: Reflection Coefficient

### 2) Mutual Coupling Enhancement

In MIMO systems, mutual coupling is the main issue. Impedance matching degradation, efficiency reduction, channel capacity reduction, correlation increase, coupling power increase, and radiation power reduction are examples of how it affects MIMO antenna characteristics (Lee et al., 2012). Many techniques exist for reducing the mutual coupling, some of which lead to single or multiband behaviours. As Figure 12 illustrates, the reflection coefficient in this configuration between the four ports is extremely tiny.

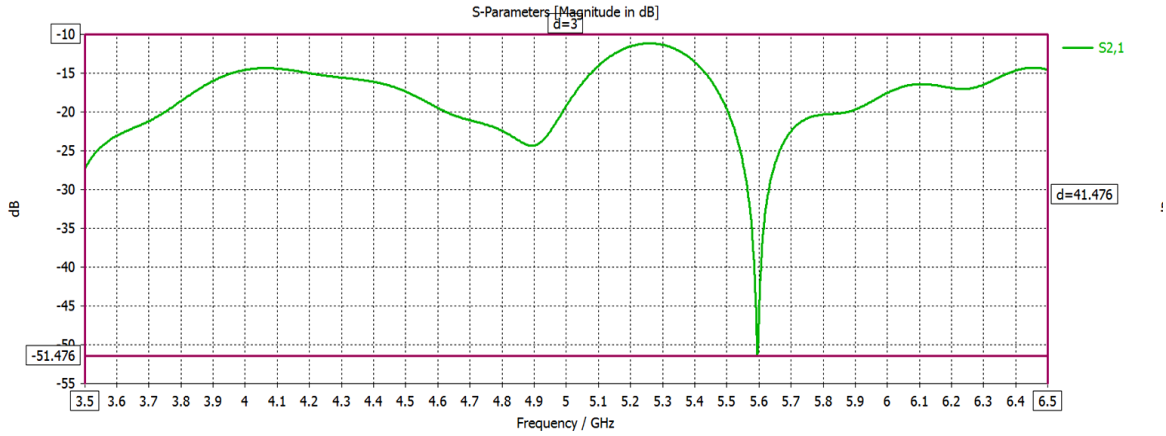

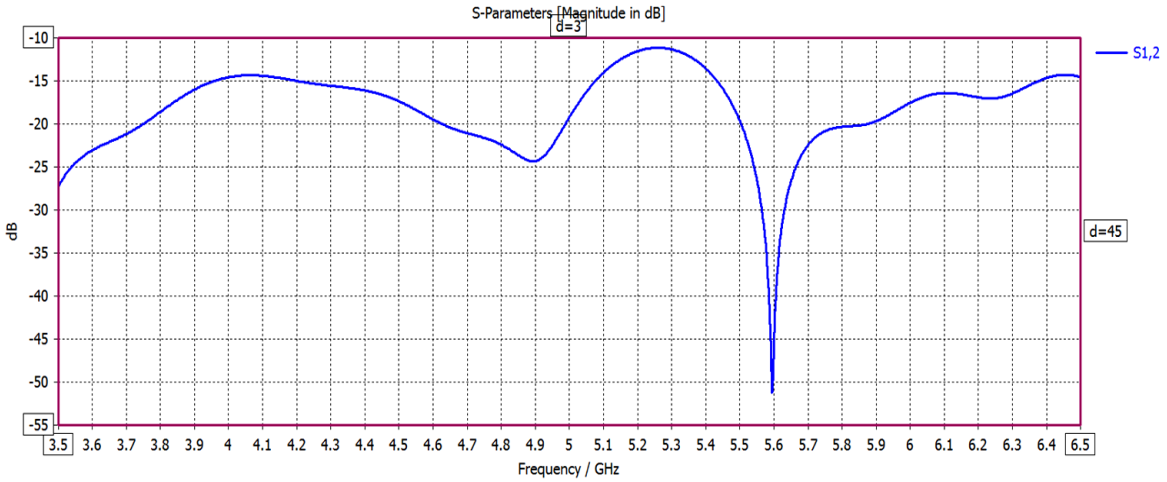


Figure 12: Reflection Coefficient: (a), $S_{12}$. (b) $S_{21}$

### 3) Voltage Standing Wave Ratio (VSWR)

The feeder line and antenna must match the feeder line to transfer the maximum amount of energy from the transmitter to the antenna. To accomplish this, the VSWR range at the antenna's intended frequency needs to be between 1 and 2 (Park & Sung, 2012). The response of VSWR against frequency is displayed in Figure 13. For frequencies of 5.6 GHz, the value of the vector signal-to-noise ratio (VSWR) is limited to 1.1509 and 1.161. This is because the majority of the signal will be transmitted while a tiny portion will experience reflection.

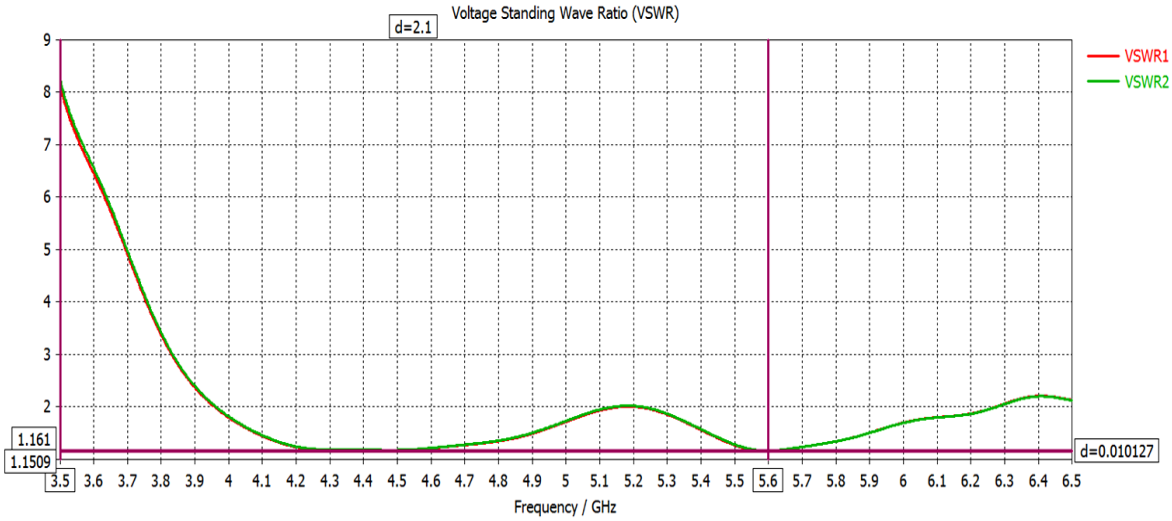


Figure 13: VSWR vs. Frequency of the Single Band Printed Question Mark Patch Antenna

### 4) Radiation Pattern

Figure 15 displays the MIMO antenna's H-plane and E-plane patterns at 5.6 frequency. This MIMO antenna's 3D radiation patterns are displayed in Figure 13 and (a) E-plane Pattern of the MIMO Antenna (b) H-plane Pattern of the MIMO Antenna shown in Figure 14.

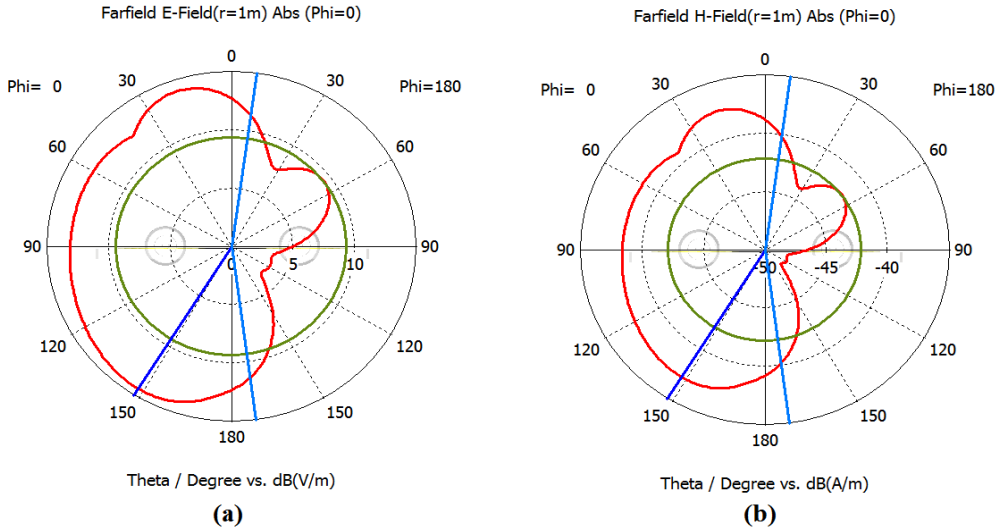


Figure 14: (a) E-plane Pattern of the MIMO Antenna (b) H-plane Pattern of the MIMO Antenna

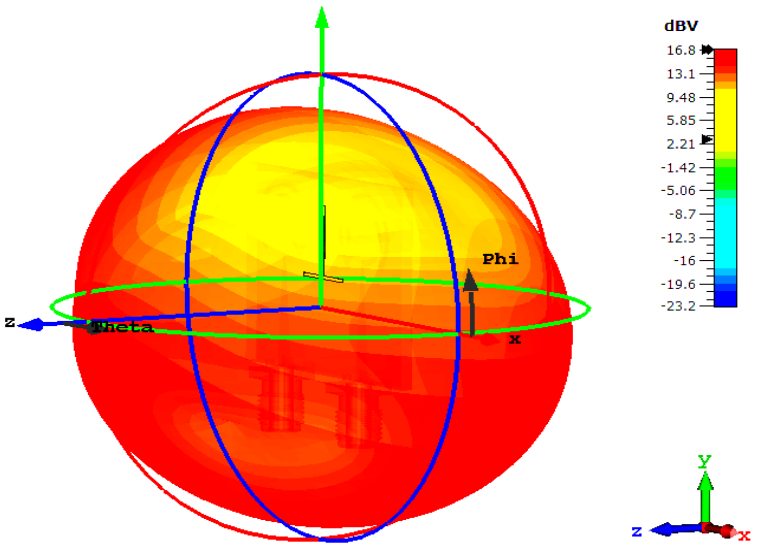


Figure 15: 3D Radiation Pattern of the MIMO Antenna

## 4 Rectifier Circuit Design

ADS software 2024 created the construction of the classical single-band rectenna, which operates at frequencies of 5G (5.6 GHz), as seen in Figure 16. Two impedance matching networks (IMN), each consisting of two capacitors and one inductor, are used in a single-band rectifier circuit to establish a resistance of 50 ohms between the antenna MIMO and the rectifier. The two HSMS-282B Schottky diodes (D4, D5) and the antenna are linked to the first IMN (L5, C8, C11). The two HSMS-282B Schottky diodes (D1, D3) and the antenna are linked to the second IMN (L2, C2, and C3). The diodes D1, D3, D4, and D5 of the HSMS-282B rectify the RF signal at 5.6 GHz. Next, a DC filter is created using capacitor C5. Parametric research was used to determine the ideal values for the DC filter, load, and components of the two IMNs. Optimum Values of Double-band Rectifier shown in Table 3.

Table 3: Optimum Values of Double-band Rectifier

| Component Name | Value | Component Name | Value |
|---|---|---|---|
| L2 | 0.3 nH | L5 | 0.968 nH |
| C2 | 400 pF | C3 | 2.212 pF |
| C8 | 400 pF | C11 | 0.39 pF |
| C5 | 1.47 pF | RL | 12 KΩ |

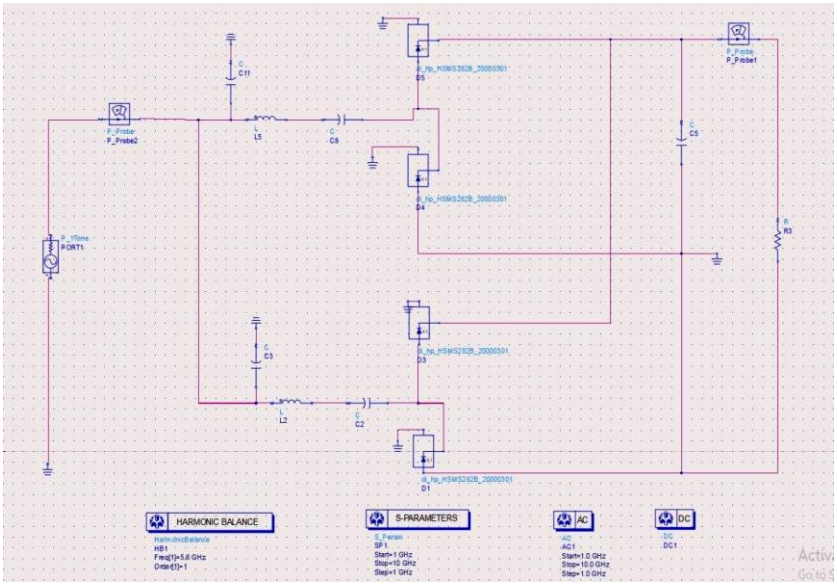


Figure 16: The Single-band Rectifier was Designed Using the Advanced Design System (ADS) Software Package

## 5 Simulation of Rectenna Design

The analysis was conducted using the ADS 2024 program software at a frequency of 5.6 GHz the following results were calculated:

a) The reflection coefficient values of the single-band rectifier circuit are found as -17 dB at 5G 5.6 GHz as shown in Figure 17. This value allows the rectifier to receive a signal of 96% from the antenna.

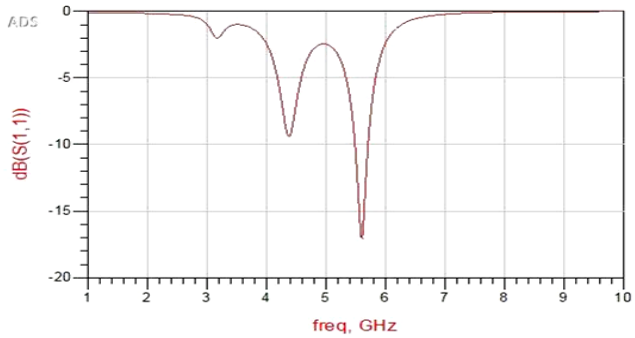


Figure 17: Reflection Coefficient vs. Frequency of the Single-band Rectifier Circuit

b) The relationship between input power and output power. When the input power changes from -30dB to +26dB, it is found that the output power changes nonlinearly, as its best value is equal to 9.1dB when the input power is 14dB when the load is fixed to 12 KΩ, as in Figure 18.

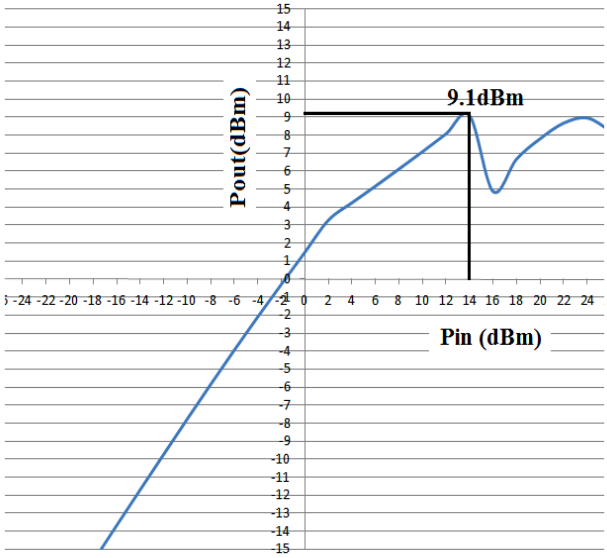


Figure 18: Input Power vs. Output Power of the Single-band Rectifier Circuit

c) The effect of load resistance on output power. It is divided into three cases according to the input power rating:

**Case 1:** When the input power was fixed to 0 dB from the antenna receiving the signal, it was found that the change in load was accompanied by a change in the output power, a nonlinear change. Also, changing the value of the load resistance in the Rectenna system changes the value of $S_{11}$. Therefore, using the Steady resistance parameter, it was found that the value of the load resistance less than 12 KΩ gives an output power less than 1.4 dB, and the value of the load resistance greater than 15 KΩ gives an output power less than 1.5 dB. The best value for the load resistance, which gives the best and greatest output capacity for the relay system, is between (12-15) KΩ, which gives 1.51 dB, as in Figure 19.

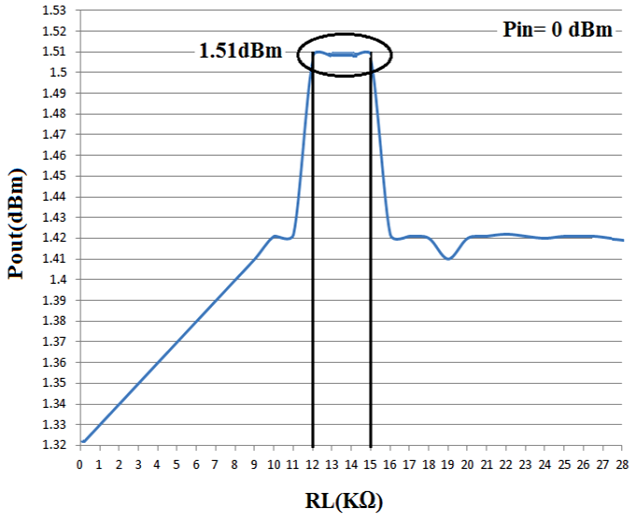


Figure 19: Output Power vs. Load Resistance at Input Power is 0 dB

**Case 2:** When the input power was fixed to 14 dB from the antenna receiving the signal, it was found that the change in load was accompanied by a change in the output power, a nonlinear change. Also, changing the value of the load resistance in the Rectenna system changes the value of $S_{11}$. Therefore, using the Steady resistance parameter, it was found that the value of the load resistance less than 12 KΩ gives an output power less than 8.994 dB, and the value of the load resistance greater than 15 KΩ gives an output power less than 9.016 dB. The best value for the load resistance, which gives the best and greatest output capacity for the relay system, is between (12-15) KΩ, which gives 9.1 dB, as in Figure 20.

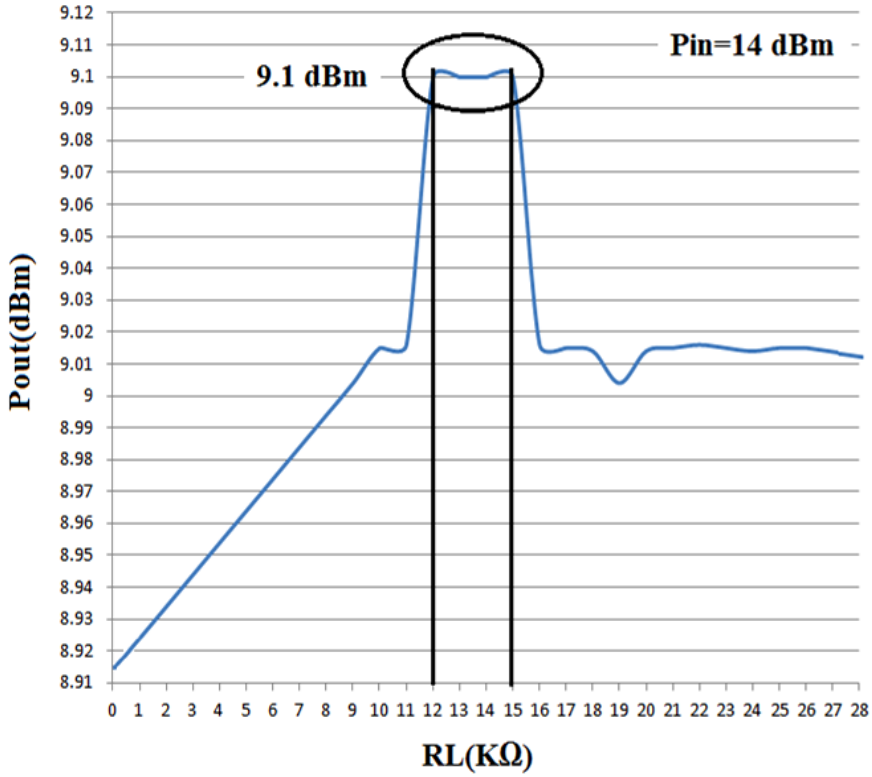


Figure 20: Output Power vs. Load Resistance at Input Power is 14 dB

**Case 3:** When the input power was fixed to 26 dB from the antenna receiving the signal, it was found that the change in load was accompanied by a change in the output power, a nonlinear change. Also, changing the value of the load resistance in the Rectenna system changes the value of $S_{11}$. Therefore, using the Steady resistance parameter, it was found that the value of the load resistance less than 12 KΩ gives an output power less than 8.133 dB, and the value of the load resistance greater than 15 KΩ gives an output power less than 8.165 dB. The best value for the load resistance, which gives the best and greatest output capacity for the relay system, is between (12-15) KΩ, which gives 8.249 dB, as in Figure 21.

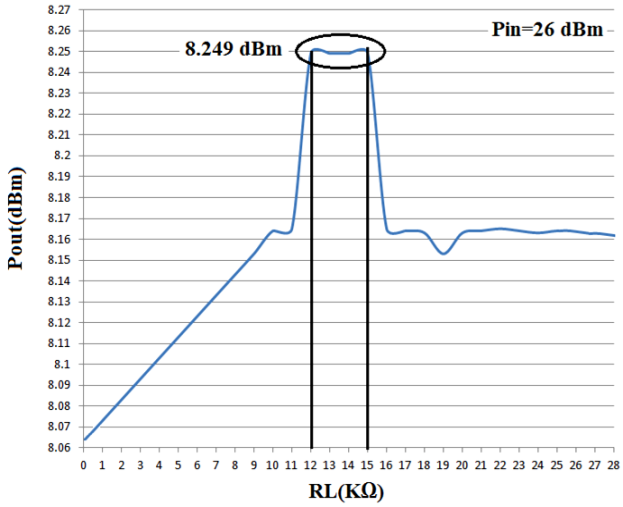


Figure 21: Output Power vs. Load Resistance at Input Power is 26 dB

From the above three cases, found that the best input power value is 14 dB, which gives the greatest output power value 9.1 dB at the resistance value of (12-15) KΩ.

a) The relationship between output voltage and current. When the input power is fixed to 14 dB, which is considered the best value to give the greatest output power, the output voltage and output current can be calculated by applying the following equations (2-3) (Wu & Ma, 2013):

$$V = \sqrt{P * R_l} \quad (2)$$

$$I = \frac{V}{R} \quad (3)$$

By changing the resistance, we notice a change in the output power when the input power is constant to 14 dB, as in Figure 20. When the load resistance increases, the output power decreases, but the output voltage increases because the relationship between the voltage, the output power, and the load resistance is direct, but an increase in resistance is much greater than a decrease. The output power therefore the output voltage increases and the output current decreases according to Ohm's law. Output Voltage vs. Output Current shown in Figure 22.

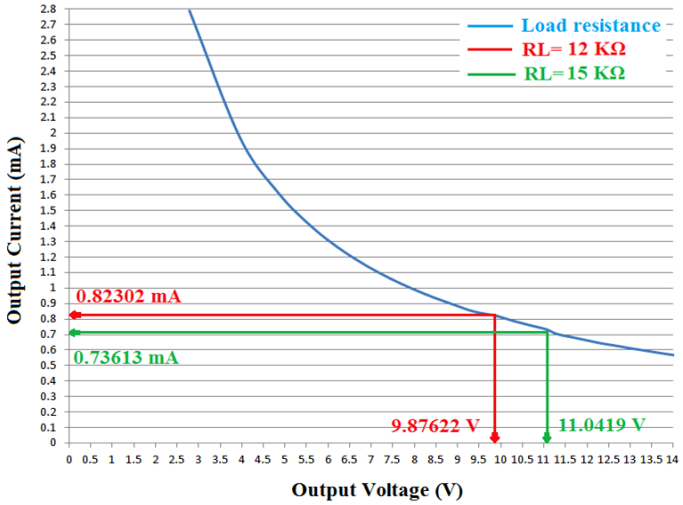


Figure 22: Output Voltage vs. Output Current

b) Conversion efficiency as a function of load resistance at a frequency of 5.6 GHz is depicted in Figure 23. The maximum conversion efficiency at this frequency is observed to be between 65% and 65.01% for load resistances ranging from 12 KΩ to 15 KΩ, with an input power of 14 dBm. Therefore, the optimal input power for the single-band rectifier at a frequency of 5.6 GHz is considered to be -14 dBm.

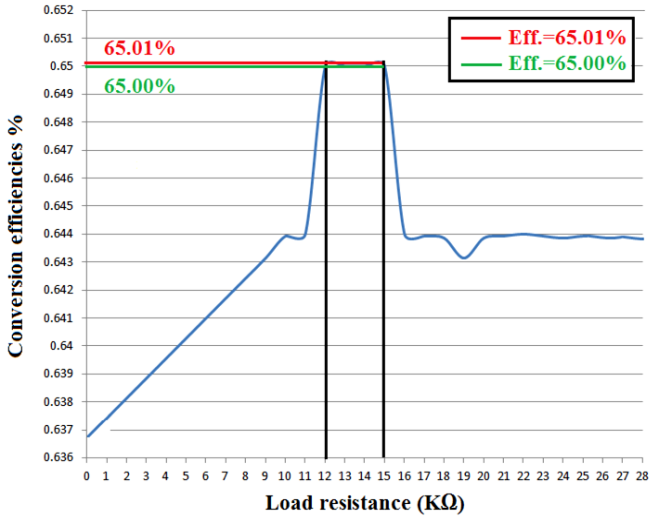


Figure 23: Simulation conversion efficiencies vs. Load resistance

Figure 24. It shows the variation of simulated conversion efficiency with frequency for the double-band rectifier at an input power of -30 dBm.

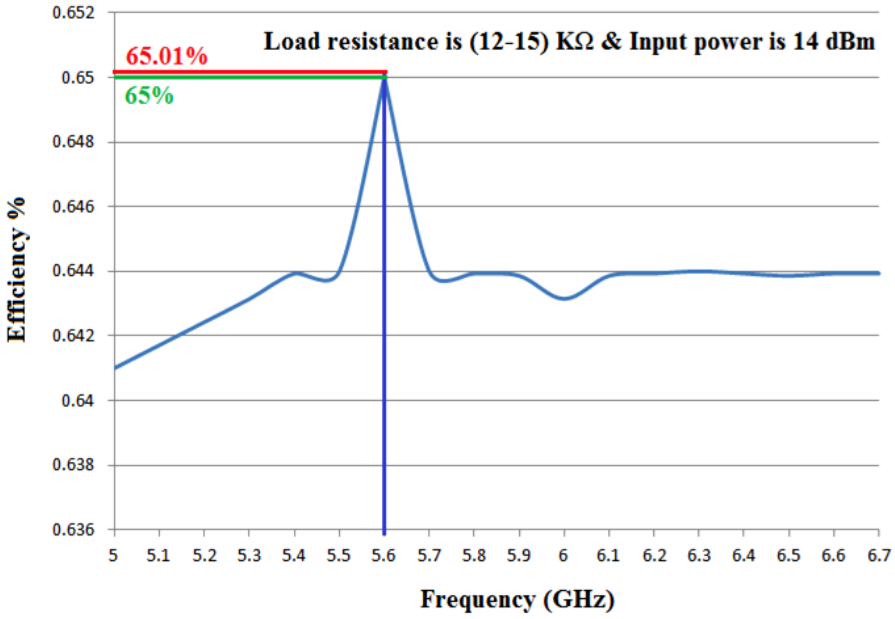


Figure 24: Variation of Conversion of Efficiency vs. Frequency of Rectifying the Circuit at an Input Power of 14 dBm and Load Resistance of (12-15) KΩ

# 6 Conclusion

Using a rectenna is a modern method for harnessing ambient microwave energy. This study presents the design and analysis of a single-band printed rectenna operating at a sub-6 frequency of 5.6 GHz. By utilizing multiple antennas, increased data rates can provide users with enhanced multimedia, real-time video connectivity, and improved data transfer capabilities. This research also discusses the design and analysis of a broadband MIMO antenna operating at 5.6 GHz for 5G applications. The total dimensions of this MIMO antenna are 30 x 40 $mm^2$, and it is printed on an FR4 substrate. The design and simulation results of this MIMO antenna were facilitated using Computer Simulation Technology (CST) in 2023. In this work, a novel design for parasitic elements is introduced, aimed at reducing mutual coupling. The parasitic elements are incorporated on the front face of the antennas, with dimensions L1 = 10 mm, L2 = 10.615 mm, W1 = 0.5 mm, and W2 = 0.6 mm, forming an upside-down letter T shape. This configuration significantly minimizes mutual coupling. Following the integration of the parasitic elements, the S-parameters were found to be $S_{11}$ = -23 dB, $S_{22}$ = -23 dB, and $S_{12}$ and $S_{21}$ = -51.545 dB at the sub-6 frequency of 5.6 GHz. This configuration effectively preserves the signal's strength, achieving a transmission and reception rate of 99%. These results are satisfactory for transmitting the signal at maximum power without compromising return power. To transfer the maximum amount of energy from the receiving antenna to the AC-to-DC converter (Schottky diode HSMS-282B) and DC filter, a rectifier circuit featuring an impedance-matching network is utilized. At an input power of 14 dBm, the maximum conversion efficiency of the rectenna at 5.6 GHz is found to be between 65% and 65.01% with a load resistance ranging from 12 KΩ to 15 KΩ. Consequently, the optimal input power for the single-band rectifier at 5.6 GHz is determined to be -14 dBm.

## Funding

There is no funding for that paper.

## Conflict of Interest

There are no conflicts of interest involved in this study.

## References

[1] Abdalla, M. A., & Ibrahim, A. A. (2017). Simple μ-negative half mode CRLH antenna configuration for MIMO applications. *Radioengineering*, *26*(1), 45-50.

[2] Ali, M., Yang, G., & Dougal, R. (2006). Miniature circularly polarized rectenna with reduced out-of-band harmonics. *IEEE Antennas and Wireless Propagation Letters*, *5*, 107-110.

[3] Alkaraki, S., & Gao, Y. (2020). Mm-wave low-cost 3D printed MIMO antennas with beam switching capabilities for 5G communication systems. *IEEE Access*, *8*, 32531-32541.

[4] Andrea, M. (2013). Array Designs for Long-Distance Wireless Power Transmission. *State-of-the-Art and Innovative Solutions. Proc. IEEE*, *101*, 6.

[5] Babu, J. K., Krishna, S. R. K., & Reddy, P. L. (2011). A review on the design of MIMO antennas for upcoming 4G communications. *International Journal of Applied Engineering Research*, *2*(1), 85.

[6] Bobir, A.O., Askariy, M., Otabek, Y.Y., Nodir, R.K., Rakhima, A., Zukhra, Z.Y., Sherzod, A.A. (2024). Utilizing Deep Learning and the Internet of Things to Monitor the Health of Aquatic Ecosystems to Conserve Biodiversity. *Natural and Engineering Sciences, 9*(1), 72-83.

[7] Brown, W. C. (1984). The history of power transmission by radio waves. *IEEE Transactions on microwave theory and techniques*, *32*(9), 1230-1242.
[8] Dahri, M. H., Abbasi, M. I., Jamaluddin, M. H., & Kamarudin, M. R. (2017). A review of high gain and high efficiency reflectarrays for 5G communications. *IEEE Access*, *6*, 5973-5985.
[9] Epp, L. W., Khan, A. R., Smith, H. K., & Smith, R. P. (2000). A compact dual-polarized 8.51-GHz rectenna for high-voltage (50 V) actuator applications. *IEEE Transactions on Microwave Theory and Techniques*, *48*(1), 111-120.
[10] European 5G Observatory. National 5G spectrum assignment. https://5gobservatory.eu/
[11] Gaurav, C., Jiyoon, K., & Vishal, S. (2018). Security of 5G-Mobile Backhaul Networks: A Survey. *Journal of Wireless Mobile Networks, Ubiquitous Computing, and Dependable Applications*, *9*(4), 41-70.
[12] Hussain, N., Jeong, M., Park, J., Rhee, S., Kim, P., & Kim, N. (2019). A compact size 2.9-23.5 GHz microstrip patch antenna with WLAN band-rejection. *Microwave and Optical Technology Letters*, *61*(5), 1307-1313.
[13] Ibrahim, H. H., Singh, M. J., Al-Bawri, S. S., Ibrahim, S. K., Islam, M. T., Alzamil, A., & Islam, M. S. (2022). Radio frequency energy harvesting technologies: A comprehensive review on designing, methodologies, and potential applications. *Sensors*, *22*(11), 4144. https://doi.org/10.3390/s22114144
[14] Khan, M. S., Iftikhar, A., Shubair, R. M., Capobianco, A. D., Asif, S. M., Braaten, B. D., & Anagnostou, D. E. (2020). Ultra-compact reconfigurable band reject UWB MIMO antenna with four radiators. *Electronics*, *9*(4), 584. https://doi.org/10.3390/electronics9040584
[15] Kim, H. (2020). 5G core network security issues and attack classification from network protocol perspective. *Journal of Internet Services and Information Security*, *10*(2), 1-15.
[16] Lee, J. M., Kim, K. B., Ryu, H. K., & Woo, J. M. (2012). A compact ultrawideband MIMO antenna with WLAN band-rejected operation for mobile devices. *IEEE Antennas and wireless propagation letters*, *11*, 990-993.
[17] Lu, P., Yang, X. S., Li, J. L., & Wang, B. Z. (2014). A compact frequency reconfigurable rectenna for 5.2-and 5.8-GHz wireless power transmission. *IEEE Transactions on Power Electronics*, *30*(11), 6006-6010.
[18] Masoodi, I. S., Ishteyaq, I., Muzaffar, K., & Magray, M. I. (2021). A compact band-notched antenna with high isolation for UWB MIMO applications. *International journal of microwave and wireless technologies*, *13*(6), 634-640.
[19] McSpadden, J. O., Yoo, T., & Chang, K. (1992). Theoretical and experimental investigation of a rectenna element for microwave power transmission. *IEEE Transactions on Microwave Theory and Techniques*, *40*(12), 2359-2366.
[20] Muhammad, S., Jiat Tiang, J., Kin Wong, S., Iqbal, A., Alibakhshikenari, M., & Limiti, E. (2020). Compact rectifier circuit design for harvesting GSM/900 ambient energy. *Electronics*, *9*(10), 1614. https://doi.org/10.3390/electronics9101614
[21] Park, Y. K., & Sung, Y. J. (2012). A Reconfigurable Antenna for Quad-Band Mobile Handset Application. *The Journal of Korean Institute of Electromagnetic Engineering and Science*, *23*(5), 570-582.
[22] Prabhu, P., Poongodi, C., Sarwesh, P., & Shanmugam, A. (2013). Design a low profile printed monopole antenna for RFID applications. *International Journal of Innovative Research in Science, Engineering and Technology*, *2*(2), 454-459.
[23] Rajesh, D., Giji Kiruba, D., & Ramesh, D. (2023). Energy Proficient Secure Clustered Protocol in Mobile Wireless Sensor Network Utilizing Blue Brain Technology. *Indian Journal of Information Sources and Services, 13*(2), 30–38.
[24] Ram, A., & Chakraborty, S. K. (2024). Analysis of Software-Defined Networking (SDN) Performance in Wired and Wireless Networks Across Various Topologies, Including Single, Linear, and Tree Structures. *Indian Journal of Information Sources and Services, 14*(1), 39–50.

[25] Ramakrishna, C., Kumar, G. S., & Reddy, P. C. S. (2021). Quadruple band-notched compact monopole UWB antenna for wireless applications. *Journal of Electromagnetic Engineering and Science*, *21*(5), 406-416.
[26] Sanad, M., & Hassan, N. (2014). Novel wideband MIMO antennas that can cover the whole LTE spectrum in handsets and portable computers. *The Scientific World Journal*, *2014*(1), 694805. https://doi.org/10.1155/2014/694805
[27] Song, C., López-Yela, A., Huang, Y., Segovia-Vargas, D., Zhuang, Y., Wang, Y., & Zhou, J. (2018). A novel quartz clock with integrated wireless energy harvesting and sensing functions. *IEEE Transactions on Industrial Electronics*, *66*(5), 4042-4053.
[28] Wu, C. H., & Ma, T. G. (2013). Self-oscillating semi-ring active integrated antenna with frequency reconfigurability and voltage-controllability. *IEEE Transactions on Antennas and Propagation*, *61*(7), 3880-3885.
[29] Wu, K., Choudhury, D., & Matsumoto, H. (2013). Wireless power transmission, technology, and applications [scanning the issue]. *Proceedings of the IEEE*, *101*(6), 1271-1275.
[30] Yang, Y., Li, J., Li, L., Liu, Y., Zhang, B., Zhu, H., & Huang, K. (2018). A 5.8 GHz circularly polarized rectenna with harmonic suppression and rectenna array for wireless power transfer. *IEEE Antennas and Wireless Propagation Letters*, *17*(7), 1276-1280.
[31] Yo, T. C., Lee, C. M., Hsu, C. M., & Luo, C. H. (2008). Compact circularly polarized rectenna with unbalanced circular slots. *IEEE Transactions on Antennas and Propagation*, *56*(3), 882-886.
[32] Zhang, Y., Lu, T., Zhao, Z., He, F., Chen, K., & Yuan, L. (2014). Selective wireless power transfer to multiple loads using receivers of different resonant frequencies. *IEEE Transactions on Power Electronics*, *30*(11), 6001-6005.
[33] Zhu, J., Hu, Z., Song, C., Yi, N., Yu, Z., Liu, Z., & Cheng, H. (2021). Stretchable wideband dipole antennas and rectennas for RF energy harvesting. *Materials Today Physics*, *18*, 100377. https://doi.org/10.1016/j.mtphys.2021.100377

## Authors Biography

**Ahmed Abdul-Kadhem Salih,** received the B.Sc. degree with first rank in Electrical and Electronics Engineering from University of Thi-Qar and M.Sc. degree in Electrical and Electronics Engineering from University of Basra, Basra, Iraq, in 2017 to 2019. PhD student in Faculty of Electrical and Computer Engineering, University of Tabriz, Tabriz, Iran Since 2021 until now. He is now an lecture in Biomedical Engineering, University of Thi-Qar, Thi-Qar, Iraq. His research interests include wireless communication, antenna and application it.

**Mahdi Nangir,** received the B.Sc. degree with first rank in Electrical Engineering from University of Tabriz and M.Sc. degree in Communication System Engineering from Sharif University of Technology, Tehran, Iran, in 2010 and 2012, respectively. He received the Ph.D. degree from K. N. Toosi University of Technology, Tehran, Iran, in 2018. In 2017, he joined McMaster University, Hamilton, Ontario, Canada as research visiting student. He is now an associate professor in Faculty of Electrical and Computer Engineering, University of Tabriz, Tabriz, Iran. His research interests include wireless communication, signal processing, multi-user information theory, code design and optimization algorithms.